



A modeling study of the SLOFEC™ Eddy Current system

Fabrice FOUCHER¹, Anouar KALAI¹, Wilhelm KELB², Salah RAMADAN³, Jérôme DELEMONTÉZ⁴

¹ EXTENDE, 15 Avenue Emile BAUDOT 91300 MASSY, France, fabrice.foucher@extende.com,
anouar.kalai@extende.com

² KONTROLL TECHNIK GmbH, Lm Laab 23, 29690 SCHWARMSTEDT, Germany, w.kelb@kontrolltechnik.com

³ KONTROLL TECHNIK GmbH Bureau France, Rue Hubert Reeves
Ecoparc Val Euromoselle F-57 140 NORROY LE VENEUR, France, s.ramadan@kontrolltechnik.com

⁴ Electricité De France - Division Technique Générale, C2M - Contrôle Matériaux Mécanismes
21 avenue de l'Europe 38040 GRENOBLE CEDEX, France, jerome.delemontez@edf.fr

Abstract: The SLOFEC™ system is a specific Eddy Current Inspection system, developed by Kontroll Technik, used industrially for the control of ferromagnetic parts and involving a partial DC magnetization of the work piece. One of the potential applications is the inspection of boiler tubes in power stations. Simulation tools can bring a significant help at different stages of NDT operations (design of the test process and the procedure, qualification, help for understanding and expertise of real inspection results, etc.). Whatever, the goal and the context of the study, the ability to vary the parameters of an inspection (having control over them) enables to minimize the number of physical trials and reduce costs while helping a better understanding of the results. In the context of the qualification of the use of the SLOFEC™ technique developed for the inspection of heat exchanger tubes in fossil-fueled power plants, EDF has engaged with EXTENDE and KONTROLL TECHNIK a simulation study of this system, in order to improve the knowledge of this technique and better estimate its potential for detection and sizing indications. The particularity of such a modelling study is to be able to simulate both the DC part and the AC part of the physical field involved with the SLOFEC™ technique. EXTENDE has conducted this simulation study with the FLUX® Finite Element package. Some results will be presented in this paper as well as some comparison with experimental data.

1. Introduction

For the inspection of heat exchanger tubes located in some coal-fired power plants, EDF has selected the SLOFEC™ inspection system developed by the company KONTROLL TECHNIK for its ability to detect corrosion pits in ferromagnetic tubes¹. In order to improve the knowledge of this technique and better estimate its potential for detection and sizing indications, EDF has engaged with EXTENDE a simulation study of this system. While helping to understand the physical principles at the basis of the SLOFEC system, the goal of this study is to validate the ability to quantitatively reproduce by simulation the results provided by the system, in order to be able to use simulation to predict the suitability of the SLOFEC (Saturation Low Frequency Eddy current) system for a given application and prepare its implementation. Indeed, the ability to change the parameters of an inspection while having a precise control of their values makes



simulation an interesting tools to prepare a real test and to minimize the number of physical trials at different stages of NDT operations (design of the test process and the procedure, qualification, help for understanding and expertise of real inspection results, etc.) and thus can reduce costs. In the first part, the SLOFEC system is presented, then the industrial applications of boiler tubes inspection is described. After a description of the specific simulation process used for the SLOFEC modeling, the different parts of the study and the results are detailed and compared to measurements: Initialization and calibration, influence of the lift-off, simulation of a realistic profile of defect. Finally, the last part of the paper relies on the different results provided by this study to help explain the physical phenomena involved in this inspection technique.

2. Presentation of the SLOFEC System

The SLOFECTM inspection system developed by the company KONTROLL TECHNIK, is composed of a DC magnetization unit, made with an electromagnet and a magnetic yoke generating a static magnetic field in the component, and of eddy current sensors operating at a given frequency located close to the outer side of the tube to be inspected. The magnetization does not aim at saturating the material but maximizing the magnetic flux in the component. With this technique, the eddy current sensors will be sensitive to the disturbance produced by a defect on the magnetic flux flowing inside the tube. In other words, the sensors will be more sensitive to a local change of permeability that will interact with the field produced by the coils, rather than the change of conductivity, since the eddy currents are really limited in a very small thickness at the external part of the tube and will not be directly disturbed by the flaw. The principle of the system is represented on figure 1.

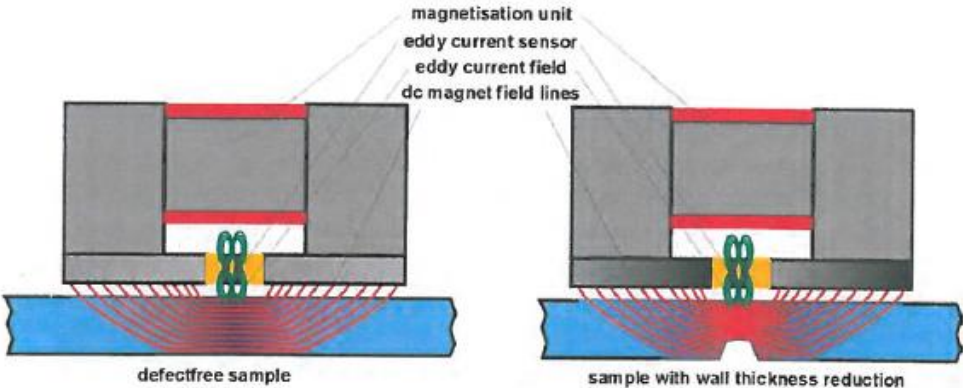


Fig 1: Principle of the inspection system

Two pictures representing the SLOFEC system and the scanner as well as another image representing the magnetization unit and a pair of eddy current sensors defined in the FLUX Finite Element software for the modelling are shown on figure 2. SLOFECTM technology offers many technical and economic advantages such as: high sensitivity detection, high inspection speed, inspection of thick wall components up to 25mm, inspection through coating up to 10mm, inspection at high temperature and distinction between topside and underside defects. The SLOFECTM is considered as fully accepted NDT technique in an increasing number of industries. Principally, the energy and oil & gas industries have had realized the advantages of

SLOFEC™ for boiler tubes, buried pipes, penstocks, tank (floor, wall, roof), vessel and drums inspection.

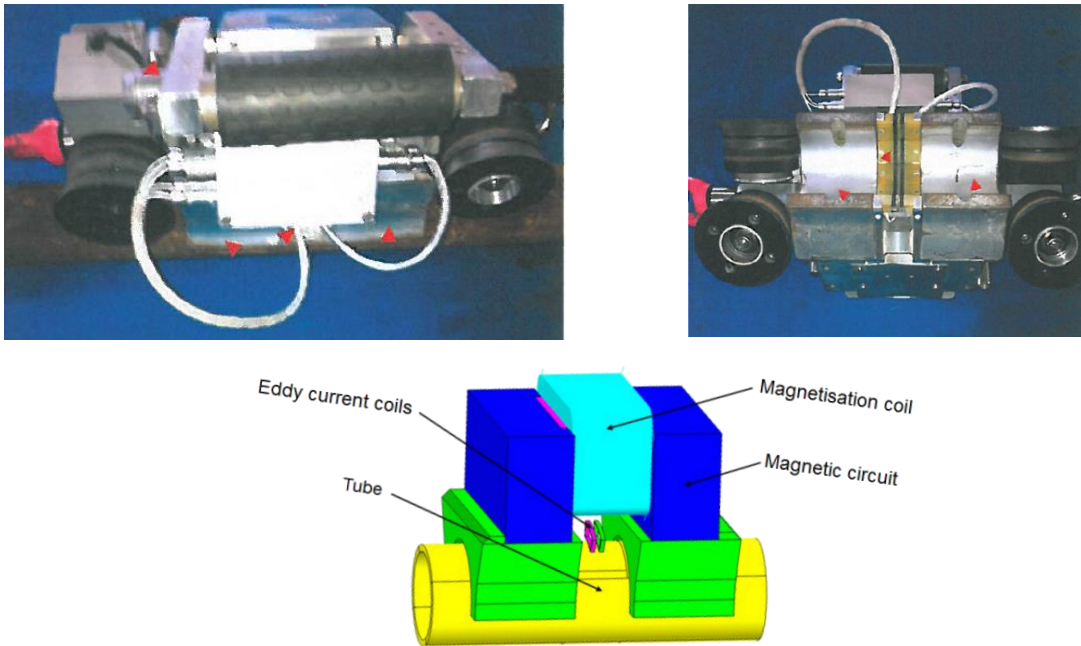


Fig 2: SLOFEC™ system and scanner:
Pictures and representation of an inspection unit in the FLUX simulation software

3. Boiler Tubes Inspection

The heater and super heater (RBT) exchangers of the 600 MW coal-fired power plants are located on the upper part of the boiler as shown in figure 3. These exchangers consist of a several tens of kilometres of tubes which diameter is 60 and 54 mm with a 4 mm wall thickness made of standard or low alloy (chromium) steel. They are essential components to furnish steam at temperatures over 600°C to the turbines. Regarding the conditions of operating, these exchangers are affected by pitting corrosion (typically cavities with a diameter of 4mm) caused by differential aeration on the internal side of the tubes which can growth very quickly and lead to leakages and tubes failures, see figure 4.

EDF decided to qualify a NDT technique applied from the external side of the tubes that could detect and locate these damages.

The SLOFEC inspection system and procedure was selected and submitted to a NDT qualification process which is defined by EDF according the European standard CEN/TR14748. This standard defines a combination of following stages:

- Some experimental trials on mock-ups with as well artificial defects as representative defects,
- Some technical justification taking account of the influence of the essential parameters.

The technical justifications consist of the study of each essential parameter regarding the influence on the sensitivity and the coverage area. The most of them were investigated under

practical tests and additionally there was a need to support this approach with numerical simulation.

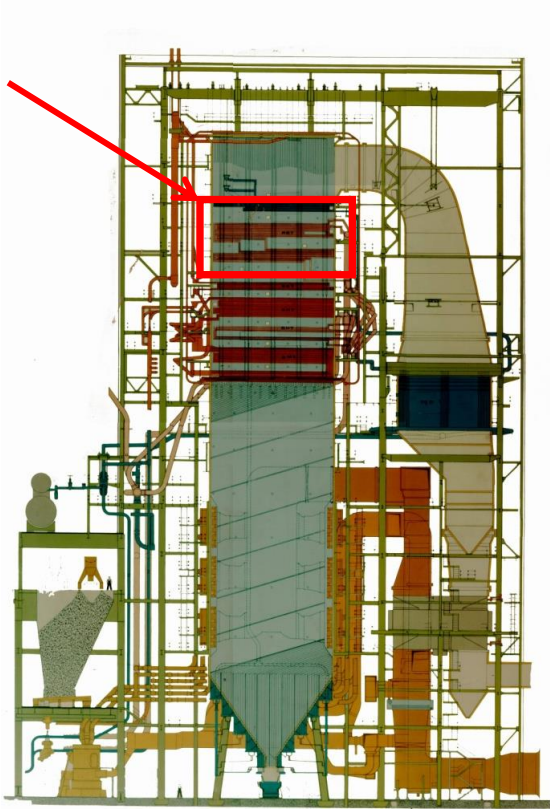


Fig. 3: Location of the RBT super heater exchangers in the coal-fired power plants

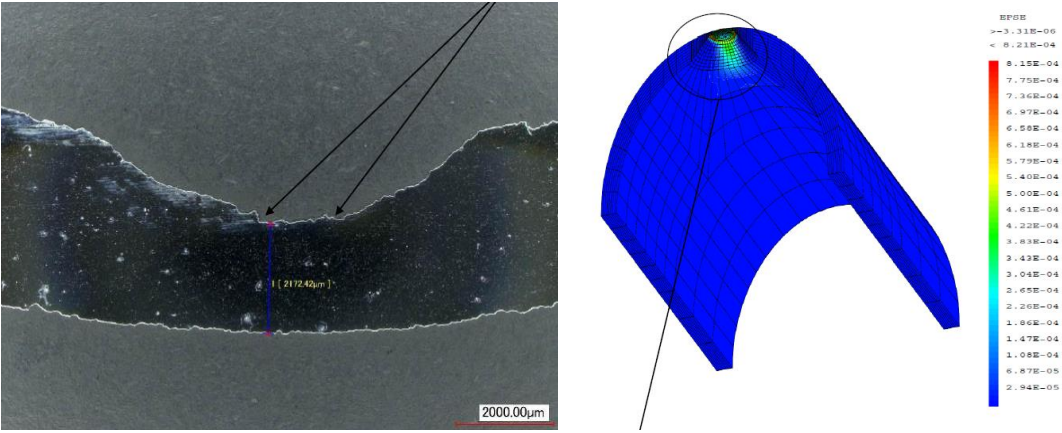


Fig. 4: example of an internal corrosion pit after metallographic I analysis – critical size of the damage defined with FEM calculation

Then, the results of the periodic NDT inspections are used to quantify the damage precisely - with local UT measurement - and to compare to a pre-calculated critical size. The main benefit regarding the implementation of a qualified and reliable NDT system is to optimize the preventive maintenance and to take the good decisions during the periodic outage to avoid the inadvertent shutdown of the power plant.

The selected test case for our simulation study deals with the inspection of RBT tubes of 60.3mm diameter and 4 mm wall thickness. These components are made of carbon steel

TU48C. The conductivity has been estimated to 6 MS/m, the magnetic permeability is not precisely known and will be estimated by reverse engineering (see part 5). The typical defects to be detected are corrosion pits, and the remaining wall thickness has to be evaluated. As a consequence, the calibration defects considered are Conical Bottom Holes (CBH) of 4mm diameter with various depths. For the RBT tube of our study, 5 CBH of 32.5% (B1), 42.5% (B2), 67.5% (B3), 77.5% (B4) and 20% (B5) depth were used for the calibration curve. These defects are represented in figure 5.

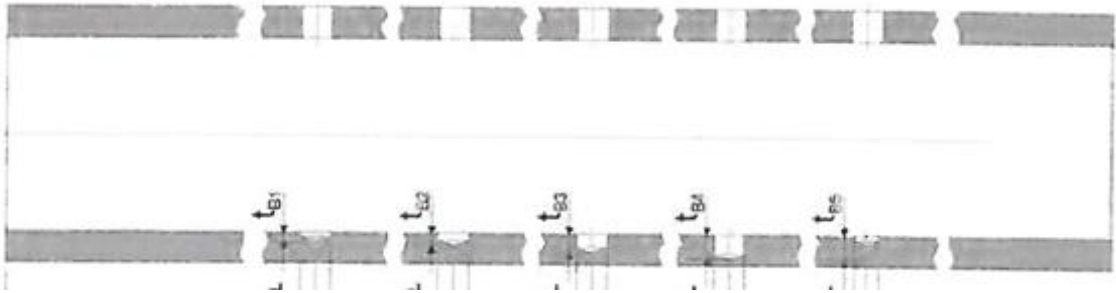


Fig. 5: Cross section of the reference tube with the 5 calibration defects B1 to B5

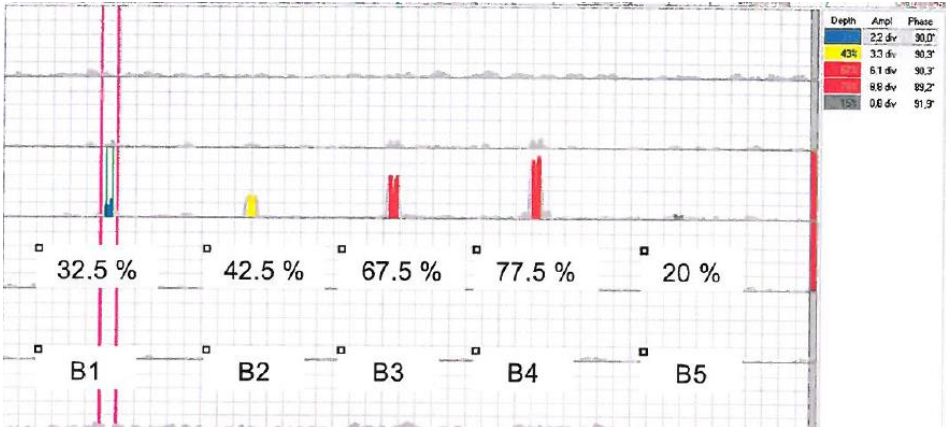


Fig. 6: Amplitude chart for the 5 flaws

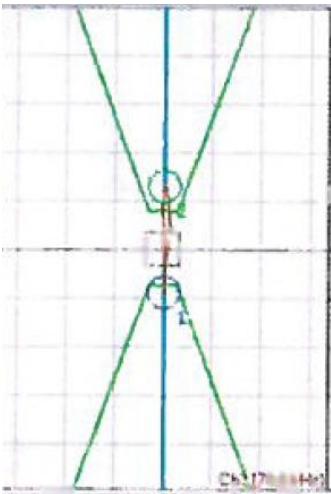


Fig. 7: Results of defect B1 in impedance plane

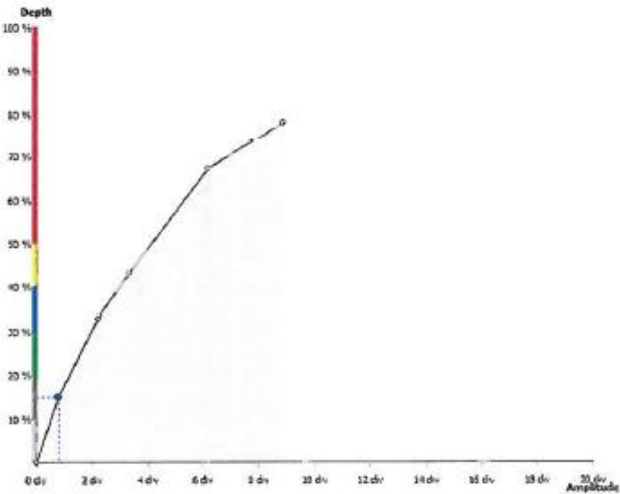


Fig. 8: Calibration curve « Amplitude / Depth »

From this calibration², a curve linking the amplitudes obtained on the defects with the SLOFEC system and their respective depths is plotted. The experimental results obtained with these

calibration defects, the signal of the defect B1 represented in the impedance plane, and finally the calibration curve Amplitude/Depth are shown on Figures 6, 7 and 8 as they appear in the acquisition software.

4. Process followed for the simulation study

As for the real inspection, the first part of a modeling study is to simulate the calibration process. Due to the strong uncertainties on the ferromagnetic properties of the tube, this calibration involved a parametric study on the material properties entered in the software allowing to fit as much as possible with the experimental calibration curve. This parametric study also allowed to verify the consistency of the results with the physical phenomena. Once this calibration and verification is performed, the influence of a variation of lift-off has been simulated. Finally, a real defect profile has been considered. These results have been compared to the measurements performed during the qualification of the SLOFEC system for this inspection.

As described above, the SLOFEC system is based on the magnetization of the part. This magnetization is performed with a DC electromagnet and leads to set the tube to a given permeability level. Once magnetized, a defect located in the tube will disturb locally the permeability of the tube (because the permeability is a function of the applied field in ferromagnetic non-saturated components) and this change of permeability distribution in the volume of the component will impact the AC magnetic field in the eddy current coils located at the outer side of the tube. With the SLOFEC technique, the coils are mainly affected by the change of material permeability due to the defect rather than the change of conductivity. Here, the DC magnetization does not reach the saturation level like in a conventional Eddy Current inspection where the goal is to homogenize the permeability distribution and increase the penetration depth of eddy currents.

In order to properly simulate the physical process, it is necessary to account for both the DC phenomenon (magnetization) and the AC phenomenon (AC field generated by the eddy currents coils). As the magnitude of the DC magnetic field is much stronger than the AC magnetic field, a reasonable assumption is to simulate separately the DC process first and then the AC process, assuming that the AC field of the eddy currents coils will not disturb noticeably the magnetization generated by the DC field (only the presence or not of a flaw will have a sensitive effect). But the AC computation needs to be performed with the precise knowledge of the local permeability distribution in the tube generated by the DC field with and without defect.

The Finite Element software, FLUX³, allows to simulate this process thanks to the so-called “Frozen permeability feature”. After having defined the magnetization curve of the material, the DC simulation allows to compute the local distribution of permeability within the volume of the tube. Then, this permeability distribution is entered as an input parameter for the material properties in the AC simulation. This AC model will then compute the eddy current signal kept by the coils. This process is repeated for each position of the scanner on the tube and done twice, once for the tube including the defect, once for the tube free of flaw. The subtraction of the signals obtained on the coils in these 2 simulations gives the defect signal while it also decreases the numerical noise produced by the mesh change due to the scanner motion in the model (this is a classical method for numerical noise reduction when using FEM software in NDT). This overall process is represented by the following graph:

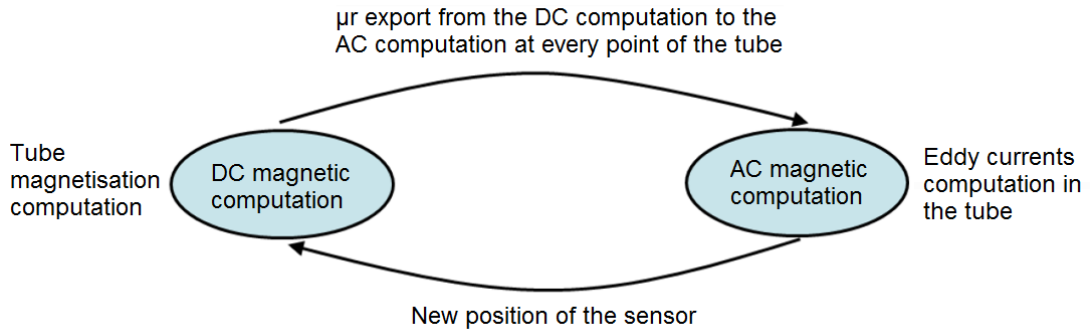


Fig. 9: Simulation process, repeated twice (with and without defect)

5. Materials properties initialization and calibration curve

These heat exchangers tubes are made of carbon steel which is a conductive and ferromagnetic material. Depending on the grade and the manufacturing process, carbon steel can exhibit very different material properties. If the conductivity can be more easily known based on literature, materials database, measurements, or at least can be estimated with a reasonable uncertainty, this is not the case for the magnetic permeability that can vary a lot between different components and is very difficult to measure. Moreover, the ferromagnetic permeability is nonlinear, i.e. depending on the magnetic field H (in A/m) applied locally, the value of the permeability will change. This ferromagnetic behavior is described with a $B(H)$ or a $\mu_r(H)$ curve for a given material where B stands for the flux density in Tesla, μ_r the relative permeability (no unit), and H for the applied magnetic field in A/m. As these properties were not known for this study, it was decided to use a reverse engineering process based on the statement that when the experimental calibration curve will be correctly reproduced by the model, the material properties selected will correspond to the real material with a good enough approximation. To reinforce the confidence in the model results, this parametric study was then accompanied with a physical reasoning on the obtained results when material parameters change (more details in the last part of this article).

The FLUX software includes different models to represent the $B(H)$ (or $\mu_r(H)$) curve of a ferromagnetic material. The more precise approach to reproduce the behavior of the material for a wide range of applied magnetic field H is to describe the curve with several points and a built-in spline interpolation function. But this approach does not allow to test easily several curves as it implies to control a lot of parameters. Moreover, the goal is not to find out the precise magnetization curve of the material for a wide range of magnetic field values but to find the best parameters to fit with the calibration curve at the operating point corresponding to our inspection. Therefore, another model of $B(H)$ curve based on only 2 parameters has been selected, well suited for a parametric study. These 2 parameters are the coefficient $\mu_{r,lin}$ and J_s , corresponding respectively to the value of the relative permeability in the “linear” part of the $B(H)$ curve (i.e. slope of the beginning of the curve), and the value of the flux density in Tesla when reaching the beginning of the saturated part of the curve. Such a curve is shown below:

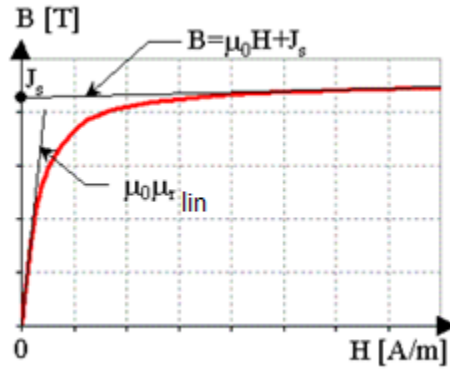


Fig. 10: Model of B(H) curve to describe ferromagnetic materials with 2 coefficients μ_{lin} and J_s

On the following graph, the calibration curve for the 3 reference defects B1, B3 and B4 obtained by the simulation are superimposed to the experimental results. This graph shows 2 sets of simulation results for 2 tests performed on the coefficients μ_{lin} and J_s among other tests that were conducted. The best fitting is obtained for $\mu_{lin}=300$ and $J_s=1.8T$ where the agreement with the calibration curve is quite good with a difference of amplitude below 10 %.

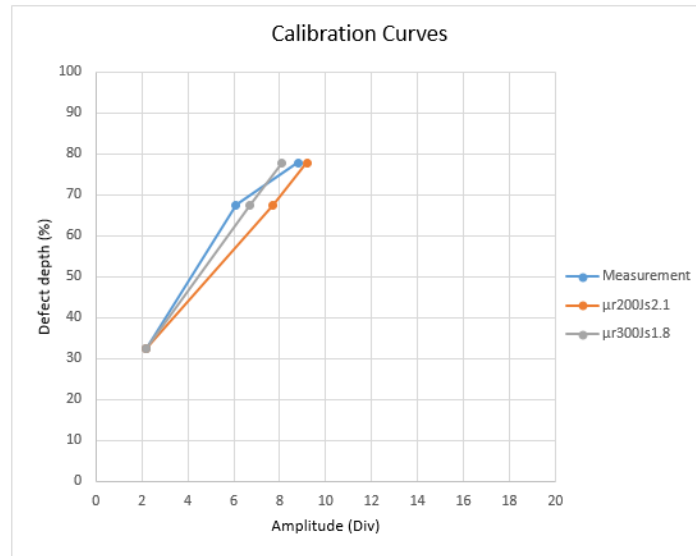


Fig. 11: Comparison Simulation/Experiment on the calibration curve

The other simulation curve presented above is for $\mu_{lin}=200$ and $J_s=2.1T$, it reaches a better “fitting” for the calibration flaw B4 (larger depth) but less for the other one. Therefore the first solution was selected to ensure a more precise model for a wide range of flaw depths. The results are summarized in the table below. An image of the signal of the defect B1 obtained by simulation is also displayed (figure 12) and looks consistent with the experimental one (figure 7).

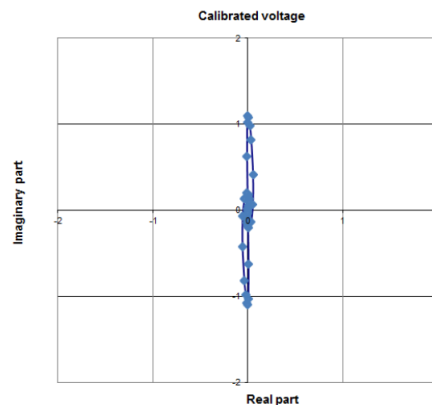


Fig. 12: Signal obtained by simulation on the defect B1

Table 1. Results on the calibration defects B1, B3 & B4

	Defect B1 (reference)		Defect B3		Defect B4	
	Ampl. (div.)	Phase (°)	Ampl. (div.)	Phase (°)	Ampl. (div.)	Phase (°)
Experiment	2,2	90°	6,1	90,3°	8,8	89,2°
Model 1 $\mu r_{lin} = 300, J_s = 1.8T$	2,2	90°	6,7	88,4°	8,1	89,3°
Model 2 $\mu r_{lin} = 200, J_s = 2.1T$	2,2	90°	7,7	88,3°	9,2	87,9°

6. Sensitivity to lift-off variation

The lift-off is one of the most influent parameters in an Eddy Current inspection. In the frame of the qualification of the inspection procedure, the impact of a variation of lift-off has been evaluated experimentally. The graph below show the results obtained experimentally for a change of lift-off between 3mm and 4.5mm for different flaw thicknesses.

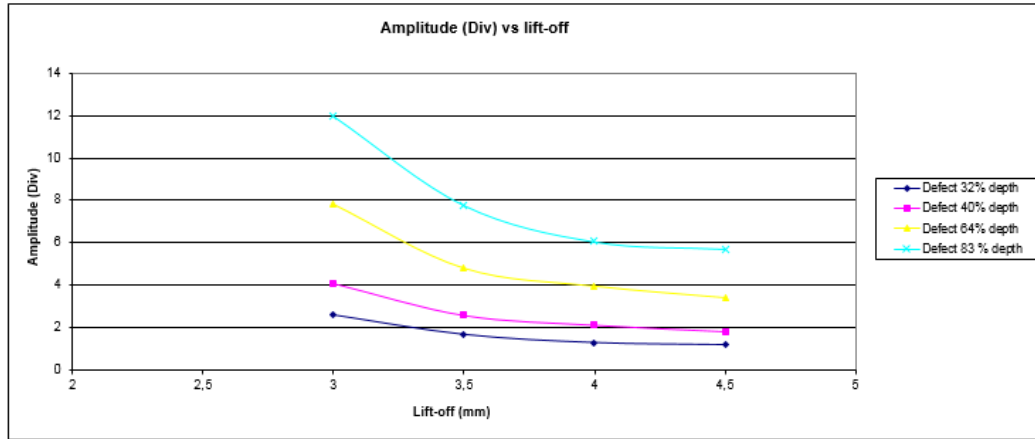


Fig. 13: Influence of the lift-off on the signal amplitude for various depths of defect (experimental results)

The amplitude drop amounts to between 52% and 56% whatever the type of defect for a lift-off variation from 3 mm to 4.5mm. The results given by the simulation on the calibration defects “B3” for these lift-off values are shown below and are consistent with these experimental measurements. The phase is unchanged while the amplitude drops from 6.7 divisions to 3.1 divisions. This corresponds to a variation of 54% as observed on the other defects experimentally.

Table 2. Influence of the lift-off on the response of the calibration flaw B3 (simulation result)

Lift-off (mm)	Amplitude	Phase
3	6,7 div.	88,4°
4,5	3,1 div.	88,3°

7. Simulation of a real defect profile

The next part of the study consisted in simulating the response of a real defect, identified as D5, corresponding to a corrosion pit. Its footprint is represented below with the color corresponding to its depth and the profile has been measured along the black axis crossing the defect center. The depth is 1.8mm (45% wall thickness) and its diameter is 9mm (radius 4.5mm). The depth

of this defect was estimated to 55% by the experimental measurement systems, whether it be the SLOFEC or the UT method as shown in the table.

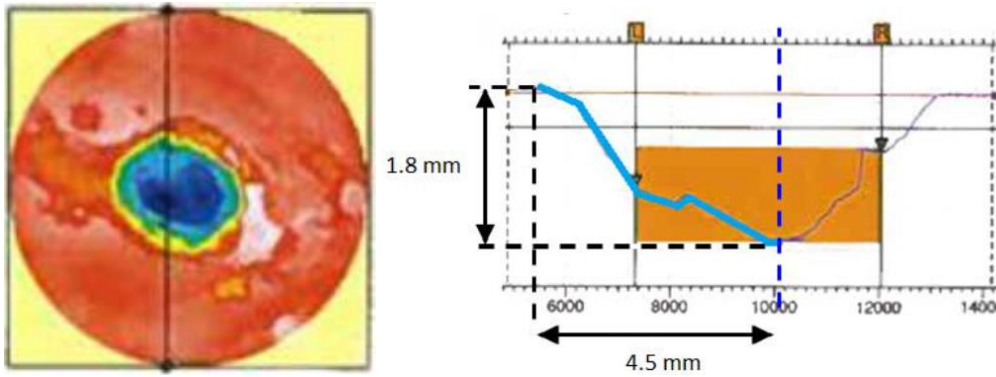


Fig. 14: Real defect profilometry

Table 3. Experimental depth estimation on the selected defect

Metrology		UT		SLOFEC	
Depth (mm)	Depth (%)	Depth (mm)	Depth (%)	Depth (mm)	Depth (%)
1,8	45	2,2	55	2,2	55

In order to see if the response of such defect could be well reproduced by simulation, this profile has been defined in the software and then the SLOFEC simulation has been simulated. The geometry and FEM mesh of the flaw model is represented in red below:

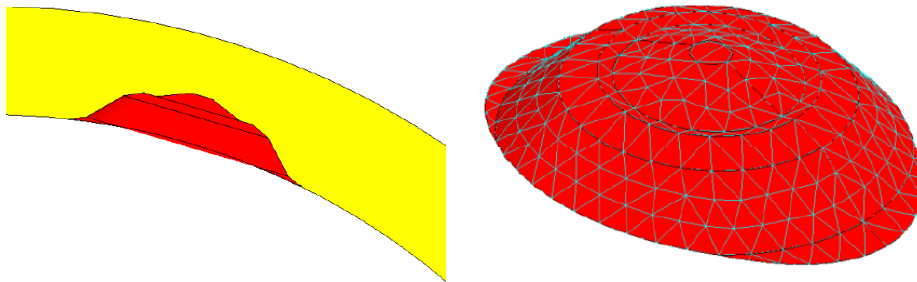


Fig. 15: Defect geometry and mesh in the FEM software

The response of this flaw in the impedance plane is shown below, the amplitude and phase is reported in the table. An amplitude of 5.1 divisions was obtained and reported on the simulated calibration curve in order to estimate the flaw depth which gave a depth of 55%, similar to the SLOFEC and UT measurements.

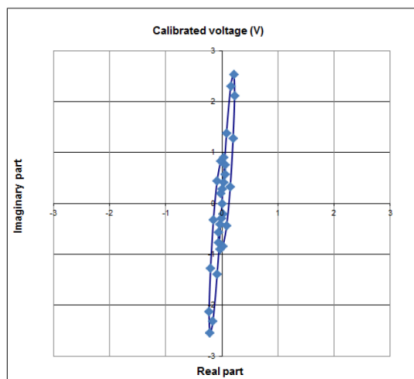


Fig. 16: Response signal of the real defect

Table 4. Simulation result on the real defect D5

Amplitude	Flaw depth estimated by simulation	Phase
5,1 div.	55%	85,3°

8. Understanding physical phenomenon thanks to simulation

8.1 Impact of a defect on the permeability distribution

As stated above, the principle of the SLOFEC inspection system relies on the perturbation generated by a defect on the local permeability in the ferromagnetic part. This change of permeability acts on the AC magnetic field seen by the eddy current sensor which produces the signal. On the images below are compared the relative permeability distribution on the inner side of the RBT tube with and without defect (the case of the real defect D5 is considered here). The color scale maximum is set to 300 on both images for the relative permeability. Without defect, the permeability is around 300 on both sides of the tube then decreases strongly around the zone center where the magnetic field generated by the magnetization unit concentrates leading to an operating point closer to the saturation level and therefore, a lower permeability. As a void defect is more reluctant than the tube to the magnetic field path, when such a defect is there, the magnetic field path is affected. As a consequence, when a wall thickness loss due to corrosion is there, it can be observed an increase of the permeability level at its sides (i.e. lower local magnetic field) and a decrease of permeability level at its top (i.e. higher magnetic field).

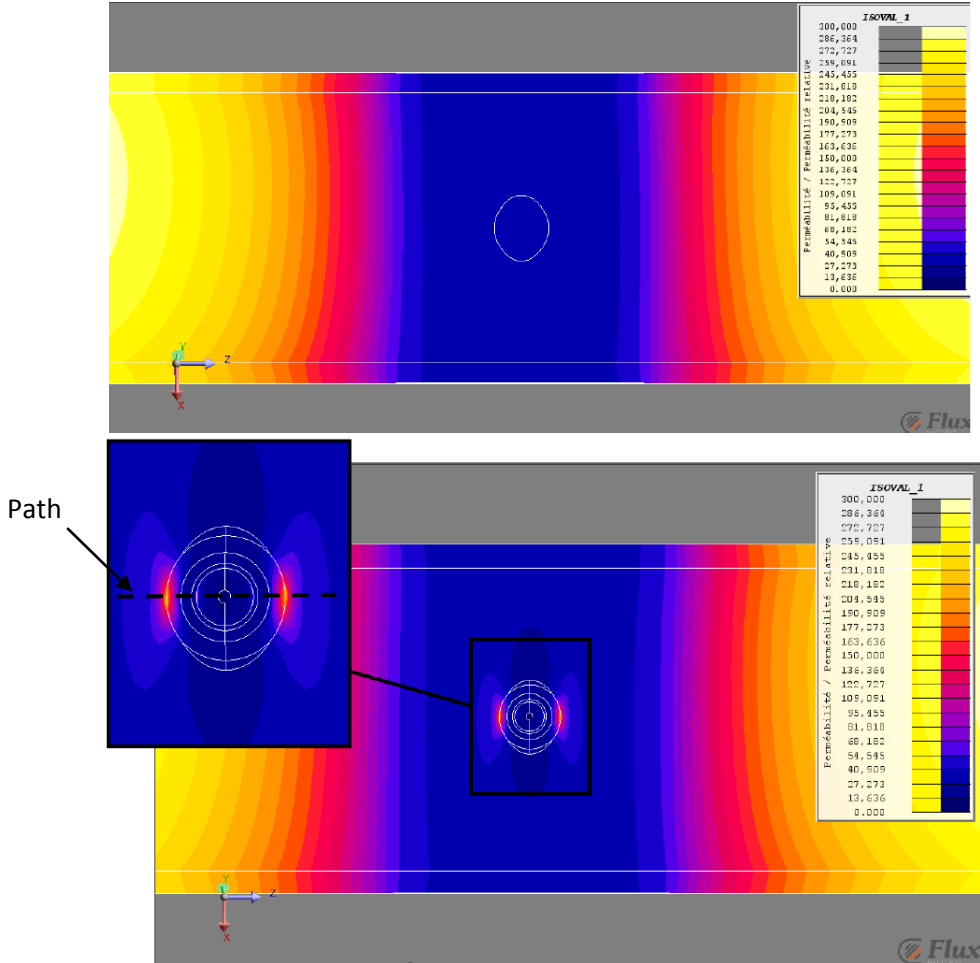


Fig. 17: Local permeability distribution without (top image) and with defect on the inner side of the tube

Then, a curve comparing the relative permeability with and without defect is shown. This curve is at 0.6mm depth in the tube section when the scanner is centered at the defect position and from the left side to the right side of the black box shown on the figure 17. The blue curve

corresponds to the permeability level without defect. The orange curve corresponds to the calibration defect B3 (67% depth, 4mm diameter) and the grey curve to the real defect D5 (45% depth, 9mm diameter). The increase and decrease of local permeability level can be clearly seen and quantified. The permeability drop on the defect is sensibly higher for the deeper defect B3 but the real defect D5 produces a permeability change on a larger distance due to its large diameter. This should accounts for the overestimation of its depth by the inspection systems, and reproduced by the simulation model.

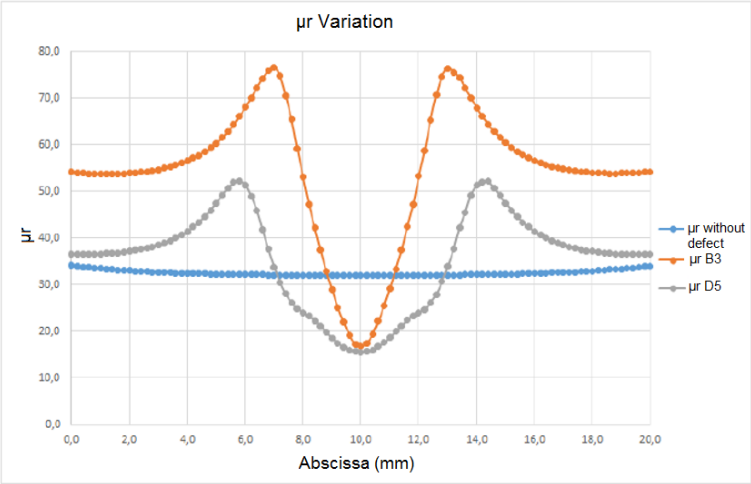


Fig. 18: Relative permeability value in the tube section

8.2 Influence of material properties

A parametric study has been conducted on the B(H) curve parameters (J_s : Flux density at saturation; μ_{lin} : relative permeability in the linear part), which also helped in our understanding and the validation of the model consistency. First, a variation of J_s from 1.6 T to 2.4 T is performed with μ_{lin} kept at 200. Then a variation of μ_{lin} from 100 to 200 is performed with J_s kept at 2.1 T, the corresponding B(H) curves are shown below:

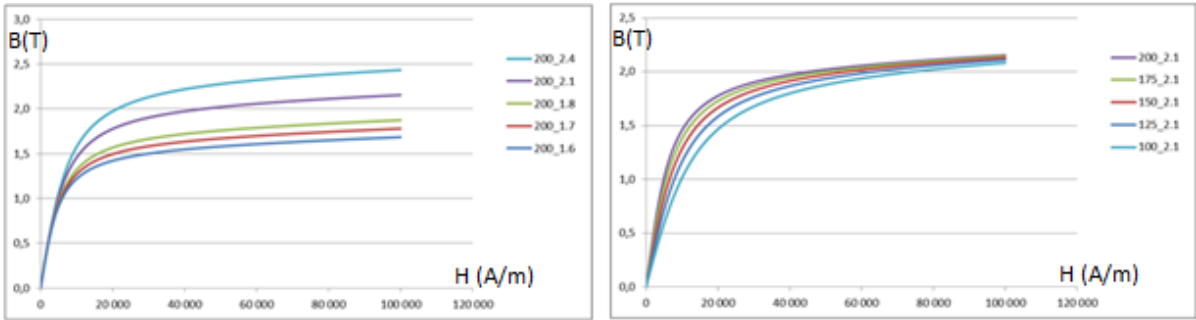


Fig. 19: B(H) curves describing tube ferromagnetic properties for different values of J_s (left image) and μ_{lin} (right image)

For a given amplitude of magnetic field applied (estimated at around 30 000 A/m around the flaw zone in our case) an increase of the material property J_s leads the tube to be further from the saturation level. At the contrary, an increase of the parameter μ_{lin} leads the tube to be closer to the saturation level in the material. The table below gives the results obtained on the calibration defect B4 for the different B(H) curve parameters tested:

Table 5. Simulation result for different B(H) curves for the tube

Variation of J_s while $\mu_{r_{in}} = 200$	1.6 T	1.7 T	1.8 T	2.1T	2.4 T
Signal amplitude on B4	8,33 div.	8,47 div.	8,63 div.	9,22 div.	9,95 div.
Variation of $\mu_{r_{in}}$ while $J_s = 2.1T$	100	125	150	175	200
Signal amplitude on B4	10,97 div.	10,54 div.	9,99 div.	9,57 div.	9,22 div.

The obtained results are consistent with our physical interpretation of the phenomenon: When the magnetization level gets closer to the saturation (case of lower J_s and of a higher $\mu_{r_{in}}$), the permeability distribution in the tube gets more homogeneous and closer to 1, therefore the defect, which has a homogeneous permeability of 1, will generate less permeability contrast, and therefore a lower signal seen by the SLOFEC system.

9. Conclusion

This paper has presented a modelling study of the inspection of ferromagnetic tubes located in heat exchangers of coal-fired power station in France by the SLOFEC system. This system, scanning on the outer side of the tube, relies on the partial magnetization of the tube with a DC magnetization unit and the effect of a defect on the tube permeability is measured by eddy current coils. The calibration curve was correctly reproduced by the simulation after a parametric study on the ferromagnetic properties of the material. Types of signals obtained were consistent also with the experiments. Then, the influence of the lift-off on the signal and depth estimation on the case of a real defect gave also a really good agreement with the measurements. The parametric analysis performed on the tube parameters and the color chart obtained on the permeability distribution also helped to understand better the physical phenomena involved in such inspection and the resultants obtained during the NDT qualification steps. The ability to reproduce with a good enough accuracy the behavior of the SLOFEC systems by a modeling tool opens the way for a larger use of simulation in this type of application: Predict the ability to detect and size a type of defect with the SLOFEC system, prepare inspection set up and optimize the system for a given application (operating frequency, coil dimensions and location of the system), help for the qualification (parametric studies on the defect and inspection parameters) are different application cases that can be conducted by simulation and which should help to implement more efficiently such types of inspection.

References

- [1] CCTP n°TAFT000PPPPRQX3028 - Cahier des charges dans le cadre des éléments du GV des chaudières Q600 et plans associés
- [2] Procédure de contrôle SLOFEC™ pour le contrôle de tubes des échangeurs RBT et SBT (SP 14.001)
- [3] <http://www.cedrat.com/en/software-solutions/flux.html>

1
2
3